CO-Induced Reductive Elimination of P(*t*-Bu)$_2$H from the Platinum(II) Dinuclear Derivative Pt$_2$[μ-P(*t*-Bu)$_2$]$_2$(H)$_2$[P(*t*-Bu)$_2$H]$_2$, Affording Mononuclear Platinum(0) or Triangulo Triplatinum(I,I,II) Derivatives

Piero Leoni,*,†,‡ Silvia Manetti,† Marco Pasquali,*,† and Alberto Albinati*,§

Dipartimento di Chimica e Chimica Industriale, Via Risorgimento 35, I-56126 Pisa, Italy, Scuola Normale Superiore, Piazza dei Cavalieri 7, I-56126 Pisa, Italy, and Istituto di Chimica Farmaceutica, Viale degli Abruzzi 42, I-20131 Milano, Italy

Received March 1, 1996[⊗]

Carbon monoxide (1 atm) quantitatively converts the Pt(II) dinuclear derivative Pt$_2$[μ-P(*t*-Bu)$_2$]$_2$(H)$_2$[P(*t*-Bu)$_2$H]$_2$ (**1**) into the new Pt$^{I}_2$Pt^{II} triangulo cluster Pt$_3$[μ-P(*t*-Bu)$_2$]$_3$(H)(CO)$_2$ (**2**). The 44e$^-$ species **2** was characterized by IR and multinuclear NMR spectroscopy and by a single-crystal X-ray diffraction study. Complex **2** is formed through the slow CO-induced reductive elimination of P(*t*-Bu)$_2$H from **1**, affording the intermediate mononuclear Pt(0) carbonyl derivative Pt[P(*t*-Bu)$_2$H]$_2$(CO)$_2$ (**4**), which equilibrates with the carbonyl-bridged triangulo derivative Pt$_3$[P(*t*-Bu)$_2$H]$_3$(μ-CO)$_3$ (**5**); these are the main products under high pressures of CO. Two alternative mechanisms were examined for the subsequent formation of complex **2**, the first being the rapid condensation of complex **4** with unreacted **1** while the second assumes **5** as the direct precursor of **2**. Although the first mechanism cannot be conclusively rejected, the second seems the most appropriate, since under high pressures of CO/H$_2$ complex **2** was shown to equilibrate with **5**. In the presence of an excess of other phosphines, the carbonylation of **1** yields quantitatively the mononuclear monocarbonyl derivatives Pt(PR$_3$)$_3$(CO) (R$_3$ = Ph$_3$, Et$_3$, *t*-Bu$_2$H).

Introduction

Since the pioneering work by Chatt and Chini,[1a] a large number of planar platinum triangulo clusters of general formula Pt$_3$(μ-L)$_3$(L′)$_3$ have been reported.[1−8] Most of them[2] have an electron count of 42 and CO, RNC, or SO_2 as bridging ligands; the terminally bonded L′ can be phosphines or, again, CO or RNC molecules. Though less common, a certain number of 44e$^-$ species are known which can be anionic, such as [Pt$_3$(μ-CO)$_3$(CO)$_3$]$^{2-}$ [3] and [Pt$_3$(μ-X)(μ-SO$_2$)$_2$(L)$_3$]$^-$,[4] cationic, such as [Pt$_3$(μ-X)(μ-PR$_2$)$_2$(L)$_3$]$^+$ (X = Cl, Br, SR, PR$_2$;[5] X = H (with NEV (number of valence electrons) = 42)[6]) or neutral, such as [Pt$_3$(μ-S)(μ-PR$_2$)$_2$(L)$_3$][5] and [Pt$_3$(μ-PR$_2$)$_3$(L)$_2$(Ph)].[7]

We report here the reaction of Pt$_2$[μ-P(*t*-Bu)$_2$]$_2$(H)$_2$[P(*t*-Bu)$_2$H]$_2$ (**1**)[8] with CO, representing a convenient access to the new neutral 44e$^-$ triangulo cluster Pt$_3$[μ-P(*t*-Bu)$_2$]$_3$(H)(CO)$_2$ (**2**). The key step of the conversion of **1** into **2** is the CO-induced reductive elimination of P(*t*-Bu)$_2$H from **1**, affording an equilibrium mixture of the mononuclear Pt(0) carbonyl derivative Pt[P(*t*-Bu)$_2$H]$_2$(CO)$_2$ (**4**) and the carbonyl-bridged triangulo derivative Pt$_3$[P(*t*-Bu)$_2$H]$_3$(μ-CO)$_3$ (**5**), which are the main products under high pressures of CO. Two different mechanisms for the subsequent formation of **1** will be presented and discussed. The alternative (depending on experimental conditions) formation of mononuclear or trinuclear derivatives with dinuclear palladium complexes as starting material has been recently reported by some of us.[9]

Complex **2**, which to our knowledge is only the second example of a Pt trinuclear derivative bearing both hydride and carbonyl ligands (the first being [Pt$_3$(μ-dppm)$_3$(μ_3-H)(μ_3-CO)]$^+$)[10] equilibrates with **5** under high pressures of CO/H$_2$.

Results and Discussion

Formation of Pt$_3$[μ-P(*t*-Bu)$_2$]$_3$(H)(CO)$_2$. A toluene suspension of the colorless Pt(II) dinuclear derivative **1** was heated at 100 °C with stirring for 3 h (eq 1) under an atmosphere of CO (1 atm). The solid slowly dissolved, giving an orange solution;

$$\underset{\mathbf{1}}{Pt_2[\mu\text{-}P(t\text{-}Bu)_2]_2(H)_2[P(t\text{-}Bu)_2H]_2} + CO \rightarrow \underset{\mathbf{2}}{Pt_3[\mu\text{-}P(t\text{-}Bu)_2]_3(H)(CO)_2} \quad (1)$$

after workup a red crystalline solid was isolated in quantitative yield and was identified as Pt$_3$[μ-P(*t*-Bu)$_2$]$_3$(H)(CO)$_2$ (**2**) by elemental analysis, IR and multinuclear NMR spectroscopy and a single-crystal X-ray diffraction study (see next section).

† Dipartimento di Chimica et Chimica Industriale.
‡ Scuola Normale Superiore.
§ Istituto di Chimica Farmaceutica.
⊗ Abstract published in *Advance ACS Abstracts,* September 15, 1996.

(1) (a) Chatt, J.; Chini, P. *J. Chem. Soc. (A)* **1970**, 1538−1542. (b) Imhof, D.; Venanzi, L. M. *Chem. Soc. Rev.* **1994**, 185−193.
(2) (a) Mingos, D. M. P.; Williams, I. D.; Watson, M. J. *J. Chem. Soc., Dalton Trans.* **1988**, 1509−1516. (b) Mingos, D. M. P.; Wardle, R. W. M. *J. Chem. Soc., Dalton Trans.* **1986**, 73−80. (c) Moor, A.; Pregosin, P. S.; Venanzi, L. M. *Inorg. Chim. Acta* **1981**, *48*, 153−157. (d) Green, M.; Howard, J. A. K.; Murray, M.; Spencer, J. L.; Stone, F. G. A. *J. Chem. Soc., Dalton Trans.* **1977**, 1509−1514. (e) Scherer, O. J.; Konrad, R.; Guggoltz, E.; Ziegler, M. L. *Chem. Ber.* **1985**, *118*, 1−21.
(3) Longoni, G.; Chini, P. *J. Am. Chem. Soc.* **1976**, *98*, 7225−7231.
(4) Bott, S. G.; Hallam, M. F.; Ezomo, O. J.; Mingos, D. M. P.; Williams, I. D. *J. Chem. Soc., Dalton Trans.* **1988**, 1461−1466.
(5) Hadj-Bagheri, N.; Browning, J.; Dehghan, K.; Dixon, K. R.; Meanwell, N. J.; Vefghi, R. *J. Organomet. Chem.* **1990**, *396*, C47−C52.
(6) Bellon, P. L.; Ceriotti, A.; Demartin, F.; Longoni, G.; Heaton, B. T. *J. Chem. Soc., Dalton Trans.* **1982**, 1671−1677.
(7) (a) Bender, R.; Braunstein, P.; Tiripicchio, A.; Tiripicchio Camellini, M. *Angew. Chem. Int. Ed. Engl.* **1985**, *24*, 861−862. (b) Bender, R.; Braunstein, P.; Dedieu, A.; Ellis, P. D.; Huggins, B.; Harvey, P. D.; Sappa, E.; Tiripicchio, A. *Inorg. Chem.* **1996**, *35*, 1223−1234.
(8) Leoni, P.; Manetti, S.; Pasquali, M. *Inorg. Chem.* **1995**, *34*, 749−752.
(9) Sommovigo, M.; Pasquali, M.; Marchetti, F.; Leoni, P.; Beringhelli, T. *Inorg. Chem.* **1994**, *33*, 2651−2656.
(10) Lloyd, B. R.; Puddephatt, R. J. *J. Am. Chem. Soc.* **1985**, *107*, 7785−7786.

S0020-1669(96)00230-3 CCC: $12.00

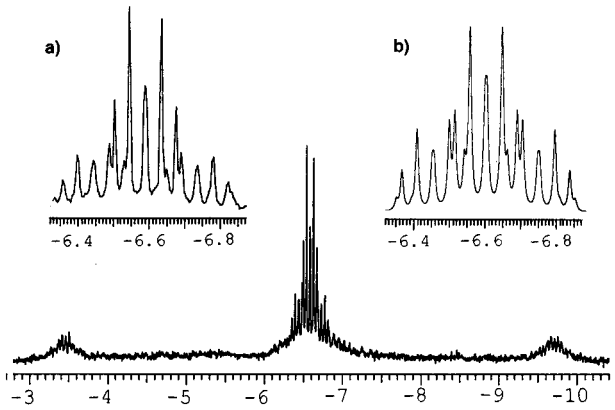

Figure 1. Portion of the ^{1}H NMR spectrum (C_6D_6, 293 K) of complex **2**, showing the hydride signal. Enlargements of the central resonances are shown in the insets: (a) experimental; (b) simulated.

Strong carbonyl stretchings were observed in the solid-state (Nujol, KBr) IR spectrum of **2** at 2001 and 1990 cm^{-1}, together with weaker absorptions at 2047, 2013, 1958, and 1942 cm^{-1}. The presence of more absorptions than those expected on the basis of the molecular geometry (see below) is probably due to solid-state effects, since the solution (DME) spectrum exhibits a single absorption at 1994 cm^{-1}. One of the weakest absorptions observed around 2000 cm^{-1} in the solid-state spectrum could be due to the ν_{PtH} vibration mode. The presence of a terminal hydride was better evidenced by the ^{1}H NMR spectrum (C_6D_6, 298 K). This consists of two doublets at 1.36 ($^3J_{HP}$ = 13.9 Hz) and 1.30 ppm ($^3J_{HP}$ = 15.3 Hz) for the *tert*-butyls and of the complex hydride signal centered at −6.60 ppm (Figure 1). The central multiplet of the latter signal, arising from isotopomer ***A*** (29%, see Chart 1), appears as a doublet of triplets due to the coupling with two equivalent (J_{HP} = 8.4 Hz) and a third (J_{HP} = 18 Hz) P nuclei. ^{195}Pt satellites from isotopomers with one ^{195}Pt nucleus were observed: a contact $^1J_{PtH}$ coupling of 1250 Hz and a long-range $^2J_{PtH}$ value of 58.8 Hz, with the satellites due to this coupling partially overlapping the central multiplet. This pattern suggests the presence of a terminally bonded hydride ligand; $^1J_{PtH}$ and $^2J_{PtH}$ for terminally bonded hydrides on dinuclear systems are in fact reported in the ranges 800−1400 and 0−300 Hz, respectively.[8]

Two signals were observed in the ^{31}P{^{1}H} NMR spectrum at 216.9 and 95.2 ppm (Figure 2) whose central lines, due to isotopomer ***A***, are a doublet and a triplet (J_{PP} = 152 Hz), respectively. Both resonances are at low fields, and the corresponding proton-coupled spectrum does not show the large $^1J_{PH}$ value characteristic of secondary phosphines. They are therefore in accord with the presence of two equivalent phosphides (P_1, P_2) coupled to a third one (P_3).

Each signal is flanked by satellites due to the presence of isotopomers ***B***−***H***. Isotopomers ***B*** and ***C*** (AA′MX spin system, A, A′ = P_1, P_2; M = P_3; X = Pt_3 (in ***B***) or Pt_1 (in ***C***)] are equivalent and give the more intense satellites (total abundance 29.6%). The M part can be analyzed with a first-order approximation and consists of a doublet of triplets centered at 95.2 ppm; the large doublet splitting corresponds to $^1J_{P_3Pt_3}$ = $^1J_{P_3Pt_1}$ = 2063.7 Hz. The A part of the subspectrum is not first order and consists of 16 lines which flank symmetrically, 8 close to and 8 distant from, the central doublet at 216.86 ppm. The simulation of this part of the spectrum gives the values of $^1J_{P_2Pt_3}$ = $^1J_{P_1Pt_1}$ = 2540.8, $^2J_{P_2Pt_1}$ = $^2J_{P_1Pt_3}$ = 116, and $^2J_{P_1P_2}$ = 163.6 Hz.

The first-order subspectrum (A_2MX spin system) due to isotopomer ***D*** (14.8%) consists of a doublet of doublets at 216.9 ppm, which gives the value $^1J_{P_1Pt_2}$ = $^1J_{P_2Pt_2}$ = 2022.5 Hz, and a doublet of triplets at 95.2 ppm, due to $^2J_{P_3Pt_2}$ = 252.8 Hz, partially overlapping the central triplet of isotopomer ***A***.

By using the values of $^1J_{Pt_1Pt_3}$ and $^1J_{Pt_1Pt_2}$ = $^1J_{Pt_2Pt_3}$, obtained by ^{195}Pt NMR spectra, and the values of J_{PP} and J_{PPt} obtained as described above, the weaker subspectra due to isotopomers ***E***−***H*** could be reproduced with good accuracy.

The ^{195}Pt{^{1}H} spectrum of **2** exhibits the two expected signals at −5611 (Pt_1, Pt_3) and −6893 (Pt_2) ppm. The signal for the two equivalent Pt_1 and Pt_3 nuclei consists of a central doublet of doublets of doublets, due to isotopomers ***B*** and ***C***, with one small ($^2J_{Pt_1P_2}$ = $^2J_{Pt_3P_1}$ = 116 Hz) and two large ($^1J_{Pt_3P_3}$ = $^1J_{Pt_1P_3}$ = 2063.7 Hz and $^1J_{Pt_3P_2}$ = $^1J_{Pt_1P_1}$ = 2540.8 Hz) couplings. Pt−Pt coupling constants were obtained by the analysis of the weaker subspectra. The equivalent isotopomers ***F*** and ***G*** give a dddd resonance, the additional coupling being $^1J_{Pt_1Pt_2}$ = $^1J_{Pt_2Pt_3}$ = 780 Hz. The value of $^1J_{Pt_1Pt_3}$ (650 Hz) was obtained by the simulation of the subspectrum due to isotopomer ***E***.

The Pt_2 signal at −6893 ppm is well-reproduced by the set of constants obtained as described above. Experimental and calculated proton-coupled ^{195}Pt spectra are reported in Figure 3; the values of $^1J_{Pt_2H}$ (1250 Hz) and $^2J_{Pt_1H}$ = $^2J_{Pt_3H}$ (58.8 Hz) which were used in the simulation, along with PPt and PtPt coupling constants from the ^{31}P{^{1}H} and ^{195}Pt{^{1}H} spectra, are in accord with those obtained by ^{1}H NMR spectra.

The ^{13}C{^{1}H} NMR spectrum exhibits broad singlets at 33.9 and 33.2 ppm (*ca*. 2:1 integral ratio) for two different types of methyl carbons and two weak multiplets at 37.7 and 39.8 ppm for the corresponding quaternary carbons. The carbonyl ligands give a weak broad resonance at 180.7 ppm.

An apparent discrepancy between the solid-state and solution structures deserves a brief comment.

X-ray diffraction shows (see next section) that complex **2** has two short (*ca*. 2.77 Å) and one long (*ca*. 3.6 Å) Pt-Pt distances. Although a strict correlation between $^1J_{PtPt}$ values and PtPt bond distances and orders is doubtful,[11,12] the solution NMR data show similar values of $^1J_{PtPt}$ coupling constants: $^1J_{Pt_1Pt_3}$ = 650 Hz and $^1J_{Pt_1Pt_2}$ = $^1J_{Pt_2Pt_3}$ = 780 Hz. Moreover, compared to P_2 and P_1, P_3 makes longer bonds (see next section) with the adjacent Pt metals but the value $^1J_{P_3Pt_1}$ = $^1J_{P_3Pt_3}$ = 2063.7 Hz is of the same order of magnitude as the remaining $^1J_{PPt}$ ($^1J_{P_1Pt_1}$ = $^1J_{P_2Pt_3}$ = 2540.8 Hz and $^1J_{P_1Pt_2}$ = $^1J_{P_2Pt_2}$ = 2036 Hz). Finally, the values of $^2J_{PP}$ are similar ($^2J_{P_1P_3}$ = $^2J_{P_2P_3}$ = 152 Hz and $^2J_{P_1P_2}$ = 164 Hz) suggesting similar P−Pt−P angles, while in the solid state the P1−Pt2−P2 angle is at *ca* 170°, *ca*. 30° wider than the P2−Pt3−P3 and P3−Pt1−P1 angles. These parameters suggest for the Pt_3 triangle an arrangement in solution more symmetrical than that observed in the solid state.

On the other hand, considering that ^{31}P chemical shifts of phosphido ligands are sensitive to M−P−M bond angles,[7b] the large difference between the values of $\delta(P_3)$ = 95.2 and $\delta(P_1)$ = $\delta(P_2)$ = 216.9 ppm favors the open-structure hypothesis. Moreover, one of the reviewers suggested that the relatively large value of $^2J_{Pt_2P_3}$ (253 Hz *vs* $^2J_{Pt_1P_2}$ = $^2J_{Pt_3P_1}$ = 152 Hz) can be explained by some through-space coupling, which is possible if the solid-state structure, with a relatively short Pt2−P3 distance (3.511(3) Å *vs* Pt1−P2 = 4.641(3) Å and Pt3−P1 = 4.634 Å), is mantained in solution.

Therefore, the matter is still open; what should be noted, however, is that this kind of complex probably has a very low barrier to Pt−Pt deformations (see later) and weak interactions could be responsible for remarkable skeletal rearrangements. For this reason the influence of solute−solvent interactions should be ruled out, since NMR spectral parameters were

(11) Pregosin, P. S. *Annu. Rep. NMR Spectrosc.* **1986**, *17*, 285−349.
(12) Pregosin, P. S. *Coord. Chem. Rev.* **1982**, *44*, 247−291.

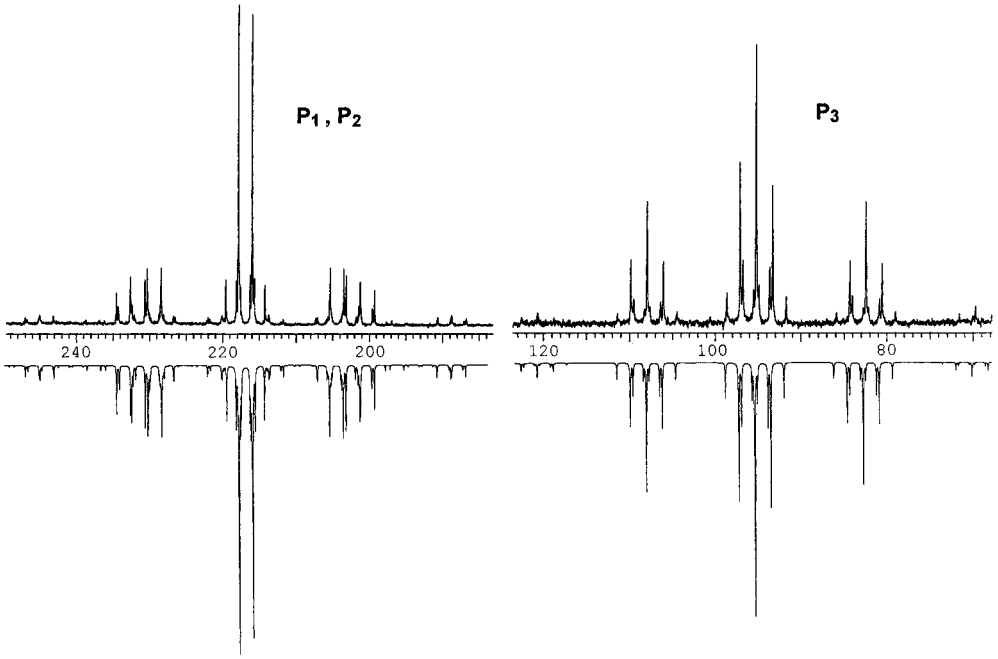

Figure 2. $^{31}P\{^1H\}$ NMR spectrum (C_6D_6, 293 K) of complex **2**: (upper trace) experimental; (lower trace) simulated.

Chart 1

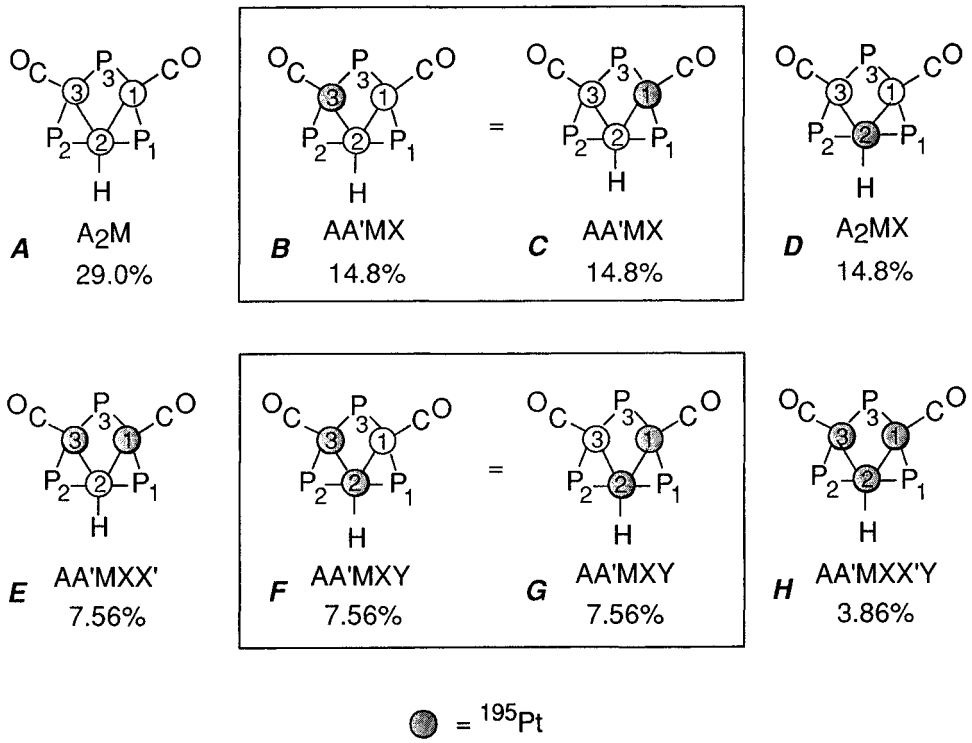

independent of the solvent (C_6D_6, $CDCl_3$, acetone-d_6); some differences between the solution and the solid-state structures, if definitely proved, should preferably be ascribed to crystal-packing forces.

Structural Study of $Pt_3[\mu\text{-}P(t\text{-}Bu)_2]_3(H)(CO)_2$ (2). The crystals of **2** contain a triangular "Pt_3" unit with two short Pt−Pt distances and a long Pt···Pt contact; each side of this unit is symmetrically bridged by a "μ-P(*t*-Bu)$_2$" group. There are two independent molecules in the asymmetric unit.

A selection of bond distances and angles for the two molecules (A and B) is given in Table 1; an ORTEP view of molecule A is shown in Figure 4.

The most significant differences between molecules A and B are (1) the Pt2−Pt3 distances at 2.7165(6) and 2.7196(6) Å, respectively, (2) the Pt1−Pt3 separations at 3.6135(6) and 3.6249 (6) Å, respectively, and (3) the P3−Pt3−C3 angles at 105.9(5) and 108.4(4)°, respectively.

Different M−M distances in chemically identical, but crystallographically non equivalent, molecules have been previously reported (especially when the separations are *ca*. 3 Å or longer). For example, in the two crystallographically independent cations found in the complex $[(PPh_3)(Ph)Pt(\mu\text{-}H)(\mu\text{-}PPh_2)Pt(PPh_3)_2](BPh_4)$,[13] the Pt−Pt distances are 2.889(1) and 2.912(2) Å, respectively, while in $[(C_5H_5)(H)W(\mu\text{-}H)Pt(Ph)(PEt_3)_2]^+$ the two M-M distances are 3.501(1) and 3.4401(1) Å, respectively.[14]

(13) Jans, J.; Nägeli, R.; Venanzi, L. M.; Albinati, A. *J. Organomet. Chem.* **1983**, *247*, C37−C41.

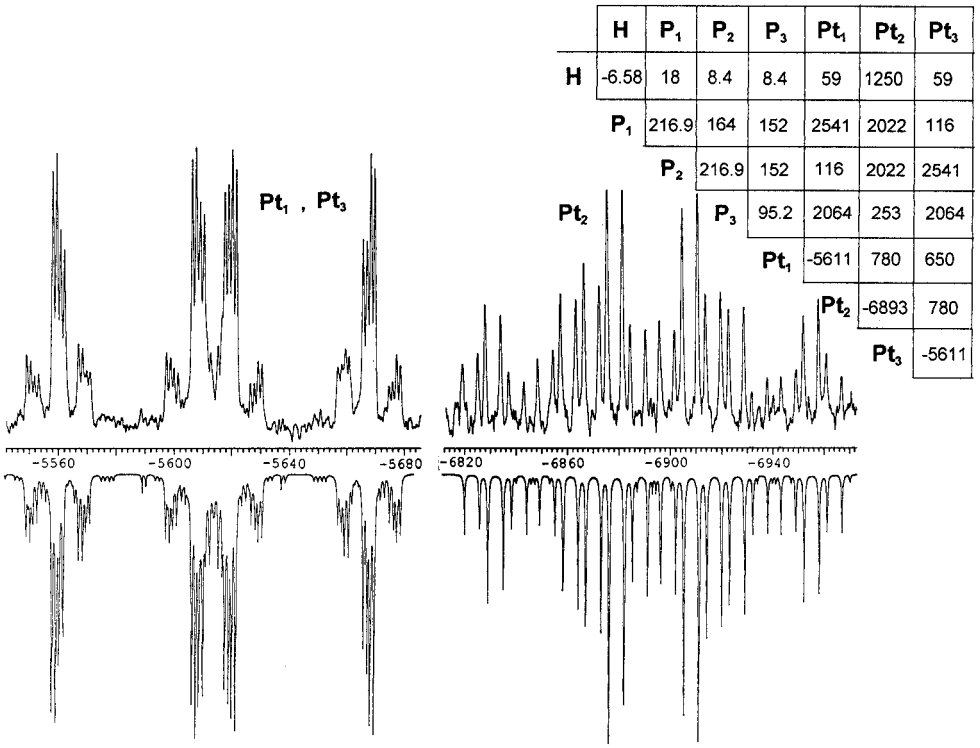

	H	P_1	P_2	P_3	Pt_1	Pt_2	Pt_3
H	-6.58	18	8.4	8.4	59	1250	59
P_1	216.9	164	152	2541	2022	116	
P_2	216.9	152	116	2022	2541		
P_3	95.2	2064	253	2064			
Pt_1	-5611	780	650				
Pt_2	-6893	780					
Pt_3	-5611						

Figure 3. Proton-coupled ^{195}Pt NMR spectrum (C_6D_6, 293 K) of complex **2:** (upper trace) experimental; (lower trace) simulated. The table shows the chemical shifts and coupling parameters used in the simulation of the spectra shown in Figures 1−3.

Table 1. Selected Bond Distances (Å) and Bond Angles (deg) for $Pt_3[\mu\text{-}P(t\text{-}Bu)_2]_3(H)(CO)_2$ **(2)**

	molecule A	molecule B
Pt1−Pt2	2.7247(6)	2.7246(6)
Pt2−Pt3	2.7165(6)	2.7196(6)
Pt1−Pt3	3.6135(6)	3.6249(6)
Pt1−P1	2.275(3)	2.281(3)
Pt1−P3	2.336(3)	2.335(3)
Pt2−P1	2.271(2)	2.273(3)
Pt2−P2	2.268(3)	2.277(3)
Pt3−P2	2.274(3)	2.272(3)
Pt3−P3	2.335(3)	2.331(3)
Pt1−C1	1.82(1)	1.87(2)
Pt3−C3	1.84(1)	1.81(1)
Pt1−Pt2−Pt3	83.23(2)	83.49(2)
Pt2−Pt1−P3	87.52(1)	87.17(7)
Pt2−Pt3−P3	87.73(7)	87.37(7)
Pt1−P3− Pt3	101.3(1)	102.0(1)
Pt1−P1− Pt2	73.65(9)	73.49(9)
Pt2−P2− Pt3	73.46(9)	73.43(9)
P1− Pt2−P2	169.6(1)	169.8(1)
P1−Pt1− P3	140.6(1)	140.7(1)
P2−Pt3− P3	140.9(1)	140.3(1)
Pt2−Pt1−C1	164.6(4)	164.8(4)
Pt2−Pt3−C3	166.3(5)	164.0(4)
P3− Pt1−C1	107.9(5)	108.0(4)
P3− Pt3−C3	105.9(5)	108.4(4)
Pt1−C1−O1	177(1)	179(1)
Pt3−C3−O3	176(2)	176(1)

Moreover, the complex $[Pt_3(\mu\text{-}PPh_2)_3(Ph)(PPh_3)_2]$ (**3**), which is isoelectronic with **2** and has an analogous "$Pt_3(\mu\text{-}PR_2)_3$" core, also shows this effect, the skeletal isomerism being induced in **3** by the presence of a clathrated solvent molecule.[7] When complex **3** is crystallized from a toluene-pentane mixture, the solid-state structure[7] is similar to that found in **2**, with short (2.758(3) Å) and long (3.586(2) Å) Pt−Pt separations, but when crystallization occurs from a CH_2Cl_2/pentane mixture, the complex is obtained as **3**·$2CH_2Cl_2$,[7] and a more regular triangular metal core is found in the solid state, with the Pt−Pt distances being 2.956(3) and 3.074(4) Å, respectively. A theoretical analysis[7b] has shown that the open and closed forms of this kind of complex differ in energy by only a few kilocalories per mole, and that the difference is minimized by the presence of a σ-donor ligand opposing the phosphido ligand which can open.

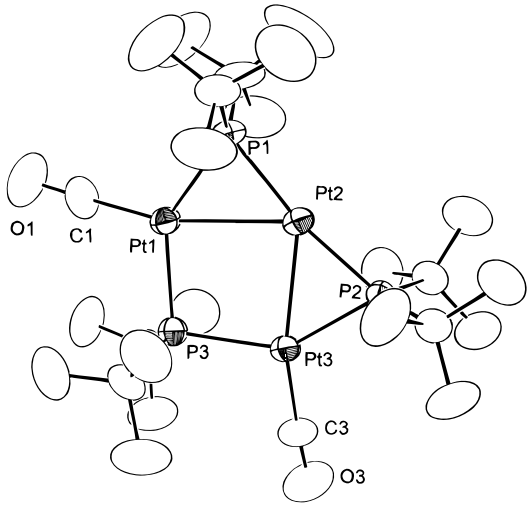

Figure 4. ORTEP plot of complex **2** (molecule A), with the atom-numbering scheme.

The different values for the Pt−Pt distances found in the two independent molecules of **2** suggest that, as previously reported for the complexes discussed above,[7,13,14] this complex has a very soft potential for the deformation of the "Pt_3" moiety. The differences in the geometries of the two molecules can be attributed to the packing forces.

The Pt1−Pt2 and Pt2−Pt3 distances (2.724 Å (average) and 2.718 Å (average)) are shorter than the sum of the metallic radii for Pt (2.78 Å)[15] and are comparable, for example, to those

(14) Albinati, A.; Nägeli, R.; Togni, A.; Venanzi, L. M. *J. Organomet. Chem.* **1983**, *330*, 85−100.

Scheme 1

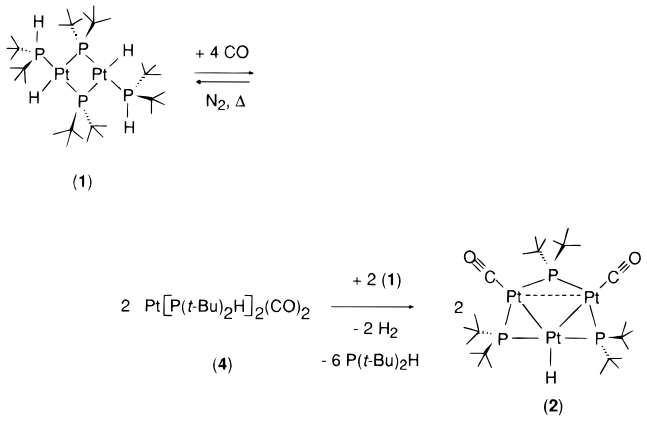

found in $[Pt_3(\mu\text{-}CO)_3\{P(C_6H_{11})_3\}_4]$[16] (2.714(1) Å) and 2.736(1) Å], or to the value of 2.758(3) Å in complex **3**.[7] Shorter separations are found in the 42e$^-$ cluster $[Pt_3(\mu\text{-}CO)_3\{P(C_6H_{11})_3\}_3]$[17] (2.654 Å (average)). The Pt1−Pt3 separation, at *ca*. 3.6 Å, is similar to the corresponding distance in **3** and is longer than the sum of the van der Waals radii (*ca.* 3.5 Å),[18] thus ruling out a Pt−Pt interaction.

As expected, there is a significant difference, in complex **2**, between the Pt−P distances of the bridging phosphido groups; the Pt−P3 distances (average 2.334(2) Å) are longer than the Pt−P separations found in the bridges spanning the shorter metal−metal separations (Pt−P1 = 2.275(4) Å (average) and Pt−P2 = 2.273(4) Å (average), respectively). Consequently, the angle at the phosphorus atom P3 is the largest (average 101.6°), and the P1−Pt2−P2 angle (169.7(1)° (average)) is larger than the P1−Pt1−P3 (140.65(7)° (average)) and P2−Pt3−P3 (140.6(4)° (average)) angles; a similar trend is also found in complex **3**.

The P atoms are approximately coplanar with the platinum atoms and the CO ligands (the deviations from the "Pt_3" plane are, in molecule A, −0.067(3) Å for P1, −0.071(3) Å for P2, and 0.119(3) Å for P3; the corresponding values for B are −0.034(2), −0.028(3), and 0.027(3) Å, respectively). Moreover, there are no significant conformational differences in the two molecules.

It proved impossible to locate the hydride ligand, but the coordination geometry around Pt2 is consistent with the expected terminal hydrido ligand.

Formation of Mononuclear Pt(0) Carbonyls. We have recently observed, in related palladium systems, that under appropriate conditions the dinuclear complex $[Pd_2(\mu\text{-}PCy_2)(\mu\text{-}\eta^3\text{-}C_3H_5)(PCy_2H)_2]$ can be converted quantitatively into trinuclear derivatives.[9] The reactions with PhEH (E = S, Se) were shown to proceed through the formation of the intermediate mononuclear complexes *trans*-$Pd(EPh)_2(PCy_2H)_2$, which, at controlled stoichiometric ratios of the reagents, condensed with their dinuclear precursor to afford the trinuclear derivatives $[Pd_3(\mu\text{-}PCy_2)_2(\mu\text{-}EPh)(PCy_2H)_2(EPh)]$.

By analogy, one could argue that the formation of the trinuclear Pt complex (**2**) proceeds as shown in Scheme 1.

The overall stoichiometry of the reaction is shown in eq 2.

$$3\,\mathbf{1} + 4CO \rightarrow 2\,\mathbf{2} + 2H_2 + 6P(t\text{-}Bu)_2H \qquad (2)$$

The mechanism proposed in Scheme 1 is of considerable interest. In the first step the dinuclear nature of the Pt(II) complex **1** is destroyed by the CO-induced intramolecular P−H reductive eliminations. If this were confirmed, complex **1** could be considered an air- and heat-stable source of the new mononuclear Pt(0) complex $Pt[P(t\text{-}Bu)_2H]_2(CO)_2$ (**4**). Both CO and $P(t\text{-}Bu)_2H$ are replaceable ligands in **4**, and a large number of new derivatives could be prepared by reacting **1** with CO in the presence of ligands suitable for Pt(0).

Although the utilization of dinuclear complexes as the precursors of mononuclear ones has frequently simpler alternatives, the above hypothesis was interesting to verify for a better understanding of the chemistry of complex **1**. Therefore, **1** was reacted with an excess of PPh_3 under a CO atmosphere. After workup $Pt(PPh_3)_3(CO)$ was isolated (68% yield) and characterized by elemental analysis and by comparison of its IR and NMR spectra with those of a sample prepared by literature methods.[19] $Pt(PEt_3)_3(CO)$ and $Pt[P(t\text{-}Bu)_2H]_3(CO)$ were also prepared by analogous reactions. The latter complexes were not isolated as solids because of their high solubilities but were identified as the unique reaction products by their solution spectra (see Experimental Section).

It is worth noting the essential role of carbon monoxide in promoting the reductive elimination of $P(t\text{-}Bu)_2H$ from **1**. In fact, when **1** was heated for 3 days at 80 °C in the presence of a large excess of PEt_3 under a nitrogen atmosphere, no traces of $Pt(PEt_3)_n$ were observed in solution, and only unreacted **1** was quantitatively recovered after workup. Thus, the reductive elimination of $P(t\text{-}Bu)_2H$ requires a precoordination of carbon monoxide to complex **1** (eq 3).

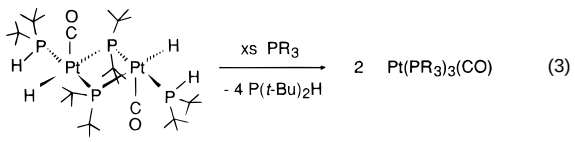

(3)

The direct proof of the intermediacy of $Pt[P(t\text{-}Bu)_2H]_2(CO)_2$ (**4**) in the formation of complex **2** was obtained by reacting **1** under 100 atm of CO in a toluene suspension, following the recommendation of one of the reviewers. After 20 h at 25 °C the reactor was depressurized and shown to contain a mixture of carbonyls and free $P(t\text{-}Bu)_2H$ (ν_{CO} (toluene) at 1979 vs and 1938 vs cm^{-1} (complex **4**)[19] and 1783 m cm^{-1} ($Pt_3(\mu\text{-}CO)_3[P(t\text{-}Bu)_2H]_3$ **5**;[19] $^{31}P\{^1H\}$ NMR (toluene, 298 K) 60.3 (very broad s, **5**), 41.9 (very broad s, **4**), 28.3 ppm (very broad s, free $P(t\text{-}Bu)_2H$), which at −70 °C respectively shift to 90.7 (broad s with Pt satellites, $^1J_{PPt}$ *ca*. 4400, $^2J_{PPt}$ *ca*. 500 Hz, **5**),[16b] 62.1 (broad s), 18.5 ppm (broad s)], which are related by an equilibrium, as reported for the analogous derivatives with tertiary phosphines.[19] This solution gives complex **2** quantitatively if warmed for 3 h at 75 °C under 1 atm of CO. If it is warmed under a nitrogen atmosphere, the solution gives back complex **1**, demonstrating that all the steps preceding the reductive elimination of H_2 are reversible.

Reaction of 1 with Mononuclear Pt^0 Derivatives. The second step of Scheme 1 is the 1/1 condensation of a Pt^{II}_2 dinuclear and a Pt^0 mononuclear derivative producing a $Pt^I_2Pt^{II}$ triangulo complex, and would deserve attention as a possible

(15) *International Tables for X-ray Crystallography*; Kluwer Academic: Dordrecht, The Netherlands, 1992; Vol. C, Chapter 9.
(16) (a) Albinati, A.; Carturan, G.; Musco, A. *Inorg. Chim. Acta* **1976**, *16*, L3−L4; (b) Moor, A.; Pregosin, P. S.; Venanzi, L. M. *Inorg. Chim. Acta* **1981**, *48*, 153−157.
(17) Albinati, A. *Inorg. Chim. Acta* **1977**, *22*, L31−L32.
(18) Bondi, A. *J. Phys. Chem.* **1964**, *68*, 441−451.
(19) Chini, P.; Longoni, G. *J. Chem. Soc. A* **1970**, 1542−1546.
(20) Sen, A.; Halpern, J. *Inorg. Chem.* **1980**, *19*, 1073−1075.
(21) MOLEN: Enraf-Nonius Structure Determination Package; Enraf-Nonius, Delft, The Netherlands, 1990.
(22) North, A. C. T.; Phillips, D. C.; Mathews, F. S. *Acta Crystallogr., Sect. A* **1968**, *A24*, 351.
(23) *International Tables for X-ray Crystallography*; Kynoch: Birmingham, England, 1974; Vol. IV.

Scheme 2

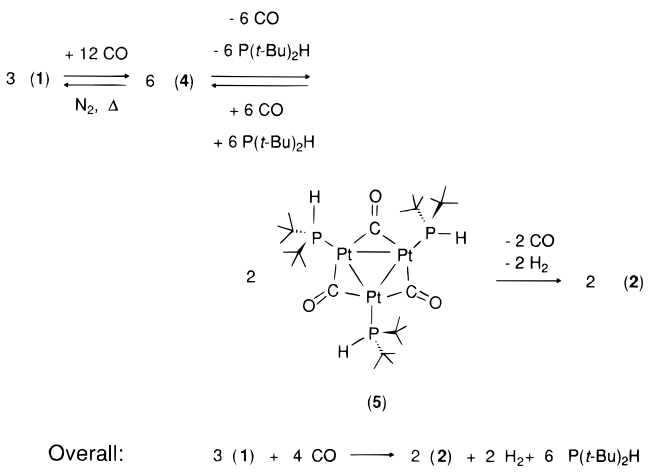

general method for the preparation of new homo- and heterometallic trinuclear systems.

The mononuclear Pt^0 reagent could only function as an electron-rich metal, which oxidatively adds the P−H bond of one of the phosphines of complex **1** to form the third phosphido ligand necessary to build up the $Pt_3[\mu\text{-}P(t\text{-}Bu)_2]_3$ core. Moreover, one molecule of H_2 should be reductively eliminated and all the remaining phosphines should be released in solution. According to this picture the mononuclear reagent can bear phosphines other than $P(t\text{-}Bu)_2H$.

To test this assumption, equimolar amounts of **1** and $Pt(PPh_3)_2(CO)_2$[19] were mixed in toluene and heated to 90 °C; the reaction was performed under either a CO or an N_2 atmosphere. The reaction under CO reached completeness after 2 h, when $^{31}P\{^1H\}$ NMR spectra of the clear orange solution showed the quantitative formation of **2**, with complete consumption of complex **1**; the other unique signals were those of free $P(t\text{-}Bu)_2H$ and PPh_3 (eq 4). The formation of molecular hydrogen was confirmed by GC analysis of the flask atmosphere.

$$\mathbf{1} + Pt(PPh_3)_2(CO)_2 \xrightarrow[\text{toluene, 90 °C}]{CO} 2 + P(t\text{-}Bu)_2H + 2PPh_3 + H_2 \quad (4)$$

The reaction performed under nitrogen gave complex **2** (36%) in a mixture with other unidentified products; a precoordination of CO to complex **1** could be relevant also in this case.

Since the reaction proceeds more selectively under CO, the presence of two CO ligands in the mononuclear reagent is nonessential, as demonstrated by the reaction of eq 5.

$$\mathbf{1} + Pt(PPh_3)_3(CO) \xrightarrow[\text{toluene, 90 °C}]{CO} \mathbf{2} + P(t\text{-}Bu)_2H + 3PPh_3 + H_2 \quad (5)$$

Alternative Mechanism. As described above, under high pressures of CO **1** gives an equilibrium mixture of $Pt[P(t\text{-}Bu)_2H]_2(CO)_2$, (**4**) and the carbonyl-bridged triangulo derivative $Pt_3(\mu\text{-}CO)_3[P(t\text{-}Bu)_2H]_3$ (**5**). This suggests an alternative pathway to the one drawn in Scheme 1 for the transformation of **1** into **2**. The oxidative addition of the P−H bonds of the secondary phosphines terminally bonded in **5** and the reductive elimination of 1 equiv of molecular hydrogen could in fact directly produce **2** (Scheme 2). The overall stoichiometry would be the same as that of eq 2.

The results of the experiments designed to support the mechanism of Scheme 1, including the reactions of **1** with the mononuclear carbonyls (eqs 4 and 5), are equally well explained by the mechanism of Scheme 2. When these reactions are performed under a CO atmosphere, complex **1** provides **4**, which gives **5** (and from the latter **2**), releasing $P(t\text{-}Bu)_2H$. The secondary phosphine substitutes PPh_3 in the mononuclear derivatives, transforming them into the equilibrium mixture of **4** and **5** and then again into **2**.

Taking into account this evidence, the mechanism of Scheme 1 cannot be ruled out conclusively, especially if one considers that all steps preceding the reductive elimination of molecular hydrogen are reversible in both schemes. However, the mechanism of Scheme 2 seems preferable, since the triangulo structure is preformed in complex **5** and its transformation into **2** requires only minor rearrangements. The reliability of this mechanism has been finally confirmed, showing that *also* the reductive elimination of H_2 can be reversed. Complex **2** was dissolved in toluene under 100 atm of a 1/1 CO/H_2 mixture. After 8 h at 25 °C the reactor was depressurized and the red solution was shown to contain a mixture of **2** and **5** (ratio 2/1 by IR and NMR) (eq 6).

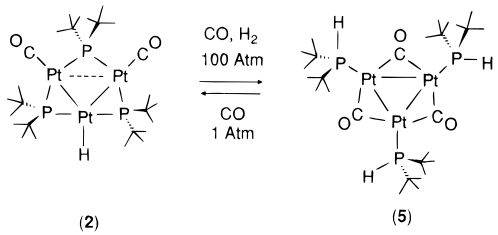

(6)

The reaction was reversed again, to quantitatively give **2**, by warming the mixture for 3 h at 75 °C under 1 atm of CO, and the cycle was repeated three times with full reproducibility.

The interesting equilibrium of eq 6 relates mixed-valence Pt^I_2-Pt^{II} and Pt^0_3 triangulo derivatives. Formally, this can occur through oxidative addition of the H−H bond, yielding a Pt^{II}_3 tris(phosphide)trihydride, followed by the reductive elimination of three P−H bonds, with the two hydrogen atoms of the H_2 molecule ending up on two phosphorus atoms. As far as we know, this is an unprecedented mechanism of H−H bond activation at transition-metal phosphido complexes. Some examples of H_2 activation assisted by terminally bonded phosphido ligands have been reported and described as heterolytic splittings induced by the high basicity of pyramidal phosphides.[24] New M−H and P−H bonds are formed in this way, along with secondary phosphines which may[24a] or may not[24b,c] remain coordinated to the metal. In some examples a reaction between H_2 and phosphido-bridged dinuclear complexes has been observed.[25] However, the reactions proceed through H_2 oxidative addition at a single metal[25c] or at the M−M bond,[25b,c] with the phosphido group behaving as a spectator ligand. Alternatively, in some cases, H_2 adds to a P−M bond, forming new P−H and M−H bonds but disrupting the dinuclear unity.[25a,b]

(24) (a) Nikonov, G. I.; Lemenovskii, D. A.; Lorberth, J. *Organometallics* **1994**, *13*, 3127−3133. (b) Roddick, D. M.; Santarsiero, B. D.; Bercaw, J. E. *J. Am. Chem. Soc.* **1985**, *107*, 4670−4678. (c) Vaughan, G. A.; Hillhouse, G. L.; Rheingold, A. L. *Organometallics* **1989**, *8*, 1760−1765.

(25) (a) Baker, R. T.; Glassman, T. E.; Ovenall, D. W.; Calabrese, J. C. *Isr. J. Chem.* **1991**, *31*, 33−53. (b) Arif, A. M.; Chandler, D. J.; Jones, R. A. *Inorg. Chem.* **1987**, *26*, 1780−1784. (c) Breen, M. J.; Duttera, M. R.; Geoffroy, G. L.; Novotnak, G. C.; Roberts, D. A.; Shulman, P. M.; Steinmetz, G. R. *Organometallics* **1982**, *1*, 1008−1010. (d) Shulman, P. M.; Burkhardt, E. D.; Lundquist, E. G.; Pilato, R. S.; Geoffroy, G. L.; Rheingold, A. L. *Organometallics* **1987**, *6*, 101−109.

Finally, a curious aspect of the equilibrium of eq 6 should be noted: in the forward direction the reaction is a $4e^-$ (furnished by the H_2 and CO molecules) reduction. However, the valence electron number decreases from 44 (in **2**) to 42 (in **5**), instead of increasing to 48. This apparent paradox is due to the fact that 6 out of 48 electrons are located on three P−H bonds which are not counted in the NEV of complex **5**.

Considering that complex **5** can still add two electrons (for tertiary phosphines the triangulo complexes $Pt_3(\mu\text{-}CO)_3(PR_3)_4$ have been reported),[1a,16,26] the $44e^-$ electron complex **2** can, in principle, add a total of 6 electrons, retaining its triangulo structure and original NEV.

Experimental Section

General Data. All manipulations were carried out under either a nitrogen or a carbon monoxide atmosphere, by using standard Schlenk techniques. High-pressure experiments were performed in an home-made 100 mL stainless steel autoclave. $Pt_2[\mu\text{-}P(t\text{-}Bu)_2]_2(H)_2[P(t\text{-}Bu)_2H]_2$ (**1**)[8] and $Pt(PPh_3)_2(CO)_2$[19] were prepared by literature methods, $P(t\text{-}Bu)_2H$ and PEt_3 (Argus Chemicals) were used as purchased. Solvents were dried by conventional methods and distilled prior to use. IR spectra (Nujol mulls, KBr) were recorded on a Perkin-Elmer FT-IR 1725X spectrometer. NMR spectra were recorded on a Varian Gemini 200 BB instrument; frequencies are referred to Me_4Si (^1H, ^{13}C), 85% H_3PO_4 (^{31}P) and H_2PtCl_6 (^{195}Pt). Simulated spectra were calculated with the program NMR″ (Version 1.0, 1989). Hydrogen evolution was detected by gas-chromatographic analyses performed with a DANI 3200 instrument equipped with a D-SM 5A column.

Preparation of $Pt(PPh_3)_3(CO)$. Complex **1** (90 mg, 0.092 mmol) was suspended in a toluene (10 mL) solution of PPh_3 (300 mg, 1.14 mmol). The colorless suspension was stirred under CO at 80°C. After 4 h the solid had dissolved; the resulting clear yellow solution was concentrated to *ca* 2 mL. After addition of n-hexane (10 mL) $Pt(PPh_3)_3$-(CO) precipitated as a yellow solid and was filtered and vacuum-dried (126.4 mg, 68% yield). IR (Nujol, KBr) 1941 cm^{-1}; lit.[19] 1942. $^{31}P\{^1H\}$ NMR: δ 12.1 (s with satellites, $^1J_{PPt} = 3536$ Hz).[20]

Preparation of $Pt(PR_3)_3(CO)$ ($R_3 = Et_3$, $(t\text{-}Bu)_2H$). Complex **1** (200 mg, 0.205 mmol) was suspended in a toluene (20 mL) solution of PEt_3 (0.15 mL, 1.02 mmol). The colorless suspension was stirred under CO at 75 °C. After 2 h the solid had dissolved, giving a clear pink solution. Due to its high solubility it was not isolated but characterized in solution. IR (Nujol, KBr): 1912 cm^{-1}; lit.[19] 1913. $^{31}P\{^1H\}$ NMR (C_6D_6, 293 K): δ −24.5 [s, uncoordinated PEt_3], −14.9 [s with satellites, $^1J_{PPt} = 3488$ Hz, $Pt(PEt_3)_3(CO)$], 15.0 [s, uncoordinated $P(t\text{-}Bu)_2H$].

$Pt[P(t\text{-}Bu)_2H]_3(CO)$ was prepared by an analogous procedure by starting with150 mg of complex **1** and a 10-fold excess of $P(t\text{-}Bu)_2H$; both reactions are practically quantitative, as inferred from the spectra.

Preparation of $Pt_3[\mu\text{-}P(t\text{-}Bu)_2]_3(H)(CO)_2$ (2). Method a. Complex **1** (300 mg, 0.307 mmol) was suspended in toluene (20 mL). Stirring the suspension for 3 h at 100°C under a CO atmosphere yielded an orange solution, which was then concentrated to *ca* 2 mL. Acetone (10 mL) was added, and complex **2** slowly precipitated as a red crystalline solid. It was filtered and vacuum-dried (215 mg, 97%). Anal. Calcd for $C_{26}H_{55}O_2P_3Pt_3$: C, 29.0; H, 5.14. Found: C, 28.9: H, 5.10. See the Results and Discussion for IR and NMR spectra.

Method b. Complex **1** (35 mg, 0.036 mmol) was suspended under a CO atmosphere in a solution of $Pt(PPh_3)_2(CO)_2$ (27.8 mg, 0.036 mmol) in toluene (2 mL). Stirring the suspension for 2 h at 90°C yielded an orange solution. The $^{31}P\{^1H\}$ NMR spectrum of the solution showed only the signals of complex **2** and free PPh_3.

High-Pressure Carbonylation of 1. Complex **1** (120 mg, 0.123 mmol) was suspended in toluene (15 mL); the suspension was transferred into a stainless steel autoclave which was then pressurized with 100 atm of CO. The suspension was stirred overnight at room temperature and was then depressurized and left under 1 atm of CO. A small amount of unreacted **1** was filtered off, and the solution was analyzed by IR and NMR spectroscopy which revealed the presence of a mixture of complexes **4** and **5** (*ca* 8/2), free $P(t\text{-}Bu)_2H$, and traces of complex **2**. IR (toluene, CaF_2): ν_{CO} at 1994 w (**2**), 1979 vs, 1938 vs (complex **4**),[19] and 1783 m cm^{-1} (complex **5**).[19] $^{31}P\{^1H\}$ NMR (toluene, 298 K): δ 60.3 br s [**5**], 41.9 br s [**4**], 23.8 br s [free $P(t\text{-}Bu)_2H$]. $^{31}P\{^1H\}$ NMR (toluene, 203 K): δ 90.7 [broad s with Pt satellites, $^1J_{PPt}$ *ca* 4400, $^2J_{PPt}$ *ca* 500 Hz, **5**],[16b] 62.1 [broad s, **4**], 18.5 [broad s, free $P(t\text{-}Bu)_2H$]. When this solution was warmed for 3 h to 75 °C under 1 atm of CO, complex **2** was isolated pure (quantitative reaction by NMR). When solutions obtained by following the same procedure were warmed for 3 h to 75 °C under a nitrogen atmosphere, complex **1** precipitated out in high yields.

Table 2. Experimental Data for the X-ray Diffraction Study of **2**

chem formula	$C_{26}H_{55}O_3P_3Pt_3$
mol wt	1077.92
T, °C	24
space group	$P2_1/c$ (No. 14)
a, Å	16.596(3)
b, Å	21.664(6)
c, Å	19.487(7)
β, deg	91.01(1)
V, Å^3	7184(3)
Z	8
ρ(calcd), g cm^{-3}	1.993
μ, cm^{-1}	119.280
λ, Å	0.710 69 (graphite monochromated, Mo Kα)
θ range, deg	$2.5 < \theta < 24.0$
no. of indep data coll	11 090
no. of obsd rflns (n_o)	7312 ($\lvert F_o\rvert^2 > 3.0\sigma(\lvert F\rvert^2)$)
transmission coeff	0.575 10−0.999 07
R[a]	0.0305
R_w[a]	0.0438

[a] $R = \Sigma(|F_o - (1/k)F_c|)/\Sigma|F_o|$ and $R_w = [\Sigma w(F_o - (1/k)F_c)^2/\Sigma_w|F_o|^2]^{1/2}$, where $w = [\sigma^2(F_o)]^{-1}$ and $\sigma(F_o) = [\sigma^2(F_o^2) + f^4(F_o^2)]^{1/2}/2F_o$.

Reaction of 2 with CO/H_2. An orange solution of complex **2** (208 mg, 0.193 mmol) in toluene (15 mL) was pressurized with 100 atm of a 1/1 mixture of CO/H_2 in a stainless steel autoclave and stirred for 8 h at 25 °C. The reactor was depressurized, and the red solution was analyzed by IR and NMR spectroscopy, which revealed the presence of a mixture of **2** and **5** (*ca.* 2/1). IR (toluene, CaF_2): ν_{CO} at 1994 vs (complex **2**) and 1783 m cm^{-1} (complex **5**); the $^{31}P\{^1H\}$ NMR of the solution exhibited the signals of complexes **2** (217 and 95 ppm) and **5** (60.3 ppm). The solution was then warmed for 12 h at 75 °C under 100 atm of the CO/H_2 mixture, cooled to room temperature, left for 4 h at 25 °C under pressure, depressurized, and analyzed as above. The ratio **2**/**5** was practically unchanged, suggesting that the equilibrium ratio had been reached after the first period under pressure.

The solution containing the mixture of **2** and **5** was then warmed for 3 h to 75 °C under 1 atm of CO and cooled to 25 °C; the IR spectrum of the orange solution exhibited a single CO stretching at 1994 vs cm^{-1} (complex **2**). The cycle was repeated three times with full reproducibility.

Crystallography. Crystals of compound **2** were obtained by crystallization from toluene. An Enraf-Nonius CAD4 diffractometer was used for the unit cell and space group determination and for the data collection. Unit cell dimensions were obtained by a least-squares fit of the 2θ values of 25 high-order reflections ($9.8 \le \theta \le 18.0°$). Selected crystallographic and other relevant data are listed in Table 2 and Table S1 (Supporting Information). Data were measured with variable scan speed to ensure constant statistical precision on the collected intensities. Three standard reflections were used to check the stability of the crystal and of the experimental conditions and measured every 1 h; no significant variation was detected. Data were corrected for Lorentz and polarization factors and for decay using the data reduction programs of the MOLEN crystallographic package.[21] An empirical absorption correction was also applied [azimuthal (Ψ) scans of 5 reflections having $\chi > 86°$].[22] The standard deviations on

(26) (a) Hidai, M.; Kokura, M.; Uchida, Y. *J. Organomet. Chem.* **1973**, *52*, 431−435. (b) Misono, A.; Uchida, Y.; Kudo, K. *J. Organomet. Chem.* **1969**, *20*, P7−P8. (c) Moor, A.; Pregosin, P. S.; Venanzi, L. M. *Inorg. Chim. Acta.* **1982**, *61*, 135−140.

intensities were calculated in term of statistics alone, while those on F_o were calculated as shown in Table 2. The structure was solved by a combination of Patterson and Fourier methods and refined by full-matrix least squares, using anisotropic displacement parameters for all atoms. The contribution of the hydrogen atoms in their idealized positions (C−H = 0.95 Å, $B = 1.5 \times B$(carbon) Å^2) was taken into account but not refined. The function minimized was: $[\sum w(|F_o| - (1/k|F_c|)^2]$ with $w = [\sigma^2(F_o)]^{-1}$. No extinction correction was deemed necessary. The scattering factors used, corrected for the real and imaginary parts of the anomalous dispersion, were taken from the literature.[23] The relevant parameters for the refinement are listed in Table 2. Upon convergence the final Fourier difference map showed no significant peaks. All calculations were carried out by using the Enraf-Nonius MOLEN crystallographic programs.[21]

Acknowledgment. The CNR (Rome) and Ministero dell'Università e della Ricerca Scientifica e Tecnologica (MURST) are gratefully acknowledged for financial support.

Supporting Information Available: Crystallographic and experimental data (Table S1), final positional and isotropic equivalent displacement parameters (Table S2), calculated positional parameters for the hydrogen atoms (Table S3), anisotropic displacement parameters (Table S4), an extended list of bond distances, bond angles, and torsion angles (Table S5), and Ortep plots showing the full numbering scheme for **2A** (Figure S1) and **2B** (Figure S2) (17 pages). Ordering information is given on any current masthead page.

IC9602308